NJC

ROYAL SOCIETY OF CHEMISTRY

PAPER

View Article Online
View Journal | View Issue

Cite this: *New J. Chem.*, 2025, **49**, 6360

Understanding the impact of additives on cobalt leaching efficiency using a citric acid-based deep eutectic solvent†

Isuri N. Perera, [a] Jennifer M. Pringle, [a] Luke A. O'Dell, [b] Amal Siriwardana [‡c] and Cristina Pozo-Gonzalo [§¶*a]

Received 27th November 2024,
Accepted 10th March 2025

DOI: 10.1039/d4nj05101g

rsc.li/njc

Recovery of critical metals such as cobalt from secondary sources is an effective way to reduce the supply risk of metals that are necessary in clean energy technologies, but such recovery processes need to be more benign. Hence, this study presents new insights into leaching cobalt using deep eutectic solvents under mild conditions. The role of ethylene glycol (EG) and water as additives in cobalt leaching was investigated using a mixture containing citric acid (CA):choline chloride (ChCl) in 1 : 1 molar ratio. While the water concentration and Co leaching efficiency were directly related, that was not the case for the EG content. A larger amount of EG in the mixture (CA : ChCl : EG from 1 : 1 : 0.3 to 1 : 1 : 4 molar ratio) decreased the cobalt leaching efficiency, which was attributed to the presence of EG in different coordination forms, as suggested by FTIR spectroscopy. The optimal solvent mixture CA : ChCl : EG (1 : 1 : 1.1) led to leaching efficiencies of 43% cobalt and 65% lithium from lithium cobalt oxide ($LiCoO_2$) at 60 °C for 48 h. Although lithium(I) was the key to increasing the leaching efficiency, we also observed that the presence of lithium(I) in the leachate could negatively impact the electrochemical reduction process. This may be due to the different speciation of cobalt(II) in the presence and absence of lithium(I), as indicated by NMR spectroscopy.

1. Introduction

The supply risk of raw and critical metals required for the manufacturing of clean energy technologies and the negative environmental impact caused by electronic devices when discarded at the end of their life cycle have generated the need for developing metal recovery strategies.[1–3] In particular, the recovery of cobalt has special consideration owing to the ethical issues associated with its primary extraction and the toxic environmental impact it causes when discarded.[4–6] The recovery of cobalt from secondary waste is mainly performed using a hydrometallurgy approach, and it generally involves 3 different steps, namely,[1] leaching, separation, and purification/recovery.[1] Sulfuric acid or nitric acid in the presence of hydrogen peroxide as a reducing agent has been extensively investigated as a leaching agent.[7–10] However, the process leads to the generation of secondary waste, including gases (chlorine, sulfur trioxide, nitric oxide and nitrogen dioxide) and acidic wastewater, which requires additional treatment, resulting in increased costs.[11]

Solvents known as deep eutectic solvents (DESs) have become popular for metal leaching (*e.g.*, cobalt) owing to their unique properties.[11–15] Many of those DESs have low cost, are easy to synthesise and biodegradable and have low volatility.[11] Generally, DESs are composed of a hydrogen bond donor (HBD) and a hydrogen bond acceptor (HBA)[11,13] and are classified into five types. Type III, which consists of a HBD and an organic salt (*e.g.*, choline chloride) as the HBA, is commonly used for metal leaching (*e.g.*, cobalt).[11] Among the reported DESs for cobalt leaching in the literature, citric acid : choline chloride (1 : 1) with 20 wt% H_2O in the presence of catalysts has shown the highest leaching efficiency (99.6%) of Co from lithium cobalt oxide ($LiCoO_2$) with a low time duration (4 h) and temperature (60 °C); however, lithium leaching was not studied under these conditions in this reported work.[16] Alternatively, water was added to decrease the viscosity in the media, and this modification was concluded to be responsible for high leaching efficiency.[16] Hua *et al.* also reported a significant increase in the leaching efficiency for cobalt and lithium when adding

[a] *Institute for Frontier Materials, Deakin University, Melbourne, Victoria 3135, Australia. E-mail: cpozo@csic.es*
[b] *Institute for Frontier Materials, Deakin University, Geelong, VIC 3216, Australia*
[c] *Tecnalia, Basque Research and Technology Alliance (BRTA), 20009 San Sebastián, Spain*

† Electronic supplementary information (ESI) available. See DOI: https://doi.org/10.1039/d4nj05101g

‡ Current address: MONOLITHOS Catalysts & Recycling Ltd., 83, Vrilissou Str., 11476 Polygono, Athens, Greece.
§ Current address: Fundación Agencia Aragonesa para la Investigación y el Desarrollo (ARAID), Av. de Ranillas 1-D, 50018 Zaragoza, Spain.
¶ Current address: Instituto de Carboquímica (ICB-CSIC), C/Miguel Luesma Castán, 4, 50018, Zaragoza, Spain.

water to an L-ascorbic acid : choline chloride 1 : 2 molar ratio system.[17] The authors reported that the addition of water reduced the viscosity of the DES, hence accelerating the transport of the reactants and products during the leaching. Nevertheless, it is also known that water can generally disrupt the DES characteristics[17] and affect its leaching properties. In principle, most of the DESs retain their hydrogen bond network structure in the presence of up to 42 wt% water.[18,19]

The existing literature primarily focuses on water as an additive to reduce viscosity in a DES. There has been limited exploration of other additives that might also reduce the viscosity while presenting a higher boiling point and avoiding additive evaporation over time. The investigation of alternative additives may provide valuable insights into the broader role of water, and enhance our understanding of its function in the cobalt leaching process.

Therefore, in this work, we investigated the role of additives in the most efficient DES for cobalt leaching, containing citric acid (CA) and choline chloride (ChCl) in a 1 : 1 molar ratio by changing the nature and concentration of additives. For that, ethylene glycol (EG) and water were investigated as additives to understand their impact on cobalt leaching. Ethylene glycol is considered as a low-toxicity chemical according to safety data sheets and literature. Furthermore, in this work, we focus on using small quantities to minimize potential exposure and reduce associated health risks.[20,21] Five leaching solvents were studied with varying amounts of EG (5.3 wt%, 20 wt% and 73 wt%) and water (5.3 wt%, 20 wt%) in CA : ChCl (1 : 1) for leaching cobalt from Co_3O_4. Additionally, $LiCoO_2$ was chosen as the cathode material to study with the most promising DES mixture composition (CA : ChCl : EG in a 1 : 1 : 1.1 molar ratio) since it only contains lithium (apart from cobalt) in the composition. We present a comprehensive analysis of speciation of cobalt(II) using our model and real leachates to understand the role of impurities and additives in the leaching process using DES.

Solvent extraction followed by chemical precipitation is the most commonly studied approach in the literature for cobalt recovery post-leaching.[16,22] However, cobalt recovery in a ''one-pot'' process, which includes electrodeposition after the leaching in the same pot, has emerged as a more environmentally sustainable alternative by reducing the amount of chemicals needed. Electrodeposition is widely used in industry as the process of choice to recover base and precious metals.[23] Therefore, cobalt electrodeposition using leachate was performed as a proof of concept in this work. Our results reveal that the electrochemical reduction of cobalt(II) is more challenging in the presence of lithium(I), as different cobalt complexes will result in the bulk.

This study provides new insights into the design of effective leaching solvents for cobalt leaching from secondary sources, and the role of additives and other metals on the leaching process. Additionally, a deeper understanding of the correlation of cobalt(II) speciation in the bulk of the leachates with the electrochemistry will contribute to the realisation of one-pot metal recovery processes.

2. Experimental

2.1. Materials and Solvents synthesis

Citric acid monohydrate with ≥99.0% purity, choline chloride with ≥98% purity, anhydrous ethylene glycol with 99.8% purity, cobalt(II, III) oxide (Co_3O_4) < 10 μm particle size, lithium cobalt(III) oxide ($LiCoO_2$) with 99.8% purity, cobalt sulfate heptahydrate ($CoSO_4 \cdot 7H_2O$) with ≥98% purity and lithium bromide (LiBr) with ≥99% purity were all purchased from Sigma-Aldrich, and used as received.

Five leaching solvents were prepared by mixing citric acid (CA) and choline chloride (ChCl) in a 1 : 1 molar ratio, and subsequently adding distilled water (H_2O) and ethylene glycol (EG) as additives under heating conditions. The composition, mass of each component and the experimental conditions are summarized in Table 1. The leaching solvents were heated and stirred at 500 rpm for different time durations (Table 1). The differences in the working conditions (temperatures and stirring durations) are based on the solubility of the components.

2.2. Co_3O_4 and $LiCoO_2$ leaching methodology

0.30 g of Co_3O_4 was added to 1.50 g of the different leaching solvents given in Table 1 to achieve a 1 : 5 solid-to-liquid ratio. All the mixtures were continuously stirred at 700 rpm at 60 °C for 72 h. 0.30 g and 0.04 g of $LiCoO_2$ (LCO) was added to 1.50 g and 2.64 g of CA : ChCl : EG (1 : 1 : 1.1) to achieve 1 : 5 and 1 : 66 solid-to-liquid ratios, respectively. The mixtures were continuously stirred at 700 rpm at 60 °C for 48 h. The leaching experiments were repeated 3 times to determine the reproducibility.

2.3. Cobalt leaching from Co_3O_4 and $LiCoO_2$ at different times

2.80 g of Co_3O_4 was added to 14.00 g of CA : ChCl : EG (1 : 1 : 1.1) to achieve a 1 : 5 solid-to-liquid ratio, and stirred at 700 rpm at 60 °C for 72 h. At different times (5 h, 10 h, 24 h, 34 h, 48 h, 58 h

Table 1 Composition of the leaching solvents, molar ratio between the components and the experimental conditions (temperature and time of stirring) used in this work

Leaching solvent	Molar ratio	CA (g)	ChCl (g)	Additive (H_2O or EG) (g)	Experimental conditions (°C, h)
CA : ChCl (1 : 1) + 5.3 wt% H_2O	1 : 1 : 1	5.5	4.0	0.5	75, 3
CA : ChCl (1 : 1) + 5.3 wt% EG	1 : 1 : 0.3	5.5	4.0	0.5	75, 3
CA : ChCl (1 : 1) + 20 wt% H_2O	1 : 1 : 4	5.5	4.0	1.9	60, 1
CA : ChCl (1 : 1) + 20 wt% EG	1 : 1 : 1.1	5.5	4.0	1.9	60, 2
CA : ChCl (1 : 1) + 73 wt% EG	1 : 1 : 4	5.5	4.0	6.9	60, 0.5

and 72 h), stirring was briefly stopped and an aliquot was removed from the solution without disturbing the solid-to-liquid ratio. 0.04 g of $LiCoO_2$ was added to 2.64 g of CA : ChCl : EG (1 : 1 : 1.1) to achieve a 1 : 66 solid-to-liquid ratio, and stirred at 700 rpm at 60 °C for 72 h. At different times (4 h, 24 h, 48 h and 72 h), stirring was briefly stopped and an aliquot was removed from the solution without disturbing the solid-to-liquid ratio.

2.4. Inductively coupled plasma mass spectrometry (ICP-MS)

The mixtures from the leaching experiments were transferred into centrifuge tubes, and centrifuged at 40 °C, 150 000 rpm for 20 minutes to separate the liquid from the unreacted solid. The temperature (40 °C) and the highest stirring rate (150 000 rpm) available in the instrument were used for an effective separation of the liquid (leachate) from the unreacted solid during the centrifugation process to ease the sample handling. Measured aliquots were taken out from the centrifuged tubes, and were diluted with 2 v/v% HNO_3 prior to the ICP-MS (PerkinElmer, USA, NexION 350X) analysis for the determination of the leached cobalt content from Co_3O_4 in each leaching solvent (Table 1) and leached cobalt and lithium contents from $LiCoO_2$ in CA : ChCl : EG (1 : 1 : 1.1). External ICP grade calibration standards were obtained through PerkinElmer, and the calibration standards for target metals were prepared in 2 v/v% HNO_3 at concentrations of 0.1, 1, 10, 100, 500 and 1000 ppb. An internal standard solution of In and Rh was used for quality control of the analysis and correction of the matrix effects.

Leaching efficiencies were calculated using the following eqn (1).[5,24,25]

$$\text{Leaching efficiency } \% = [C \times V/X] \times 100 \quad (1)$$

C = concentration of the metal leached (mg L^{-1}), V = Volume of the leaching solvent (L), X = Weight of the metal present in the solid (mg)

2.5. Dynamic viscosity

The dynamic viscosities of the leaching solvents (Table 1) were measured with an Anton Paar Lovis (Austria) 200ME viscometer using the rolling ball method at 60 °C. A capillary of 2.5 mm diameter was used with an angle of 50° for the leaching solvents with EG and H_2O as additives in a molar ratio of 1 or < 1, and with an angle of 24° for the leaching solvents consisting of EG and H_2O in a molar ratio of 4, respectively, depending on the fluidity. In addition, the dynamic viscosities of the two leachates using Co_3O_4 and $LiCoO_2$ (leached using CA : ChCl : EG (1 : 1 : 1.1)) were measured at 60 °C and an angle of 50° using the same capillary (2.5 mm diameter). The dynamic viscosity at 60 °C was calculated using the density of the leaching solvent, which was measured with an Anton Paar DMA4500 densitometer at 60 °C.

2.6. Ionic conductivity

The ionic conductivities of the leachates from Co_3O_4 and $LiCoO_2$ (leached using CA : ChCl : EG (1 : 1 : 1.1) were measured using a Biologic MTZ-35 Analyser. A dip cell made with two Pt electrodes was used for measuring the conductivity of the leachates. The cell was inserted in a brass block containing cartridge heater, which was connected to the Eurotherm 2204 temperature controller. Data were collected from a frequency range of 10 MHz to 1 Hz with a voltage amplitude of 0.1 V from 60 °C to 30 °C, and the leachates were held at each temperature for 20 minutes until they became stable. Two heating and cooling curves were conducted for reproducibility. The cell constant was obtained using 0.01 mol L^{-1} KCl at 30 °C (using the known conductivity = 0.001547 S cm^{-1}), following the equation below.

$$G^* = R \times \sigma \quad (2)$$

G^* = cell constant (Ω mS cm^{-1}), R = resistance (Ω), σ = conductivity (mS cm^{-1}).

Then, the obtained cell constant was used to calculate the conductivity of the leachates using the same equation.

2.7. Fourier transform infrared (FTIR) spectroscopy

The FTIR spectra of two leaching solvents (CA : ChCl : EG in 1 : 1 : 1.1 and 1 : 1 : 4 molar ratios), leachates from Co_3O_4 and 0.5 mol L^{-1} $CoSO_4{\cdot}7H_2O$ dissolved in these two leaching solvents were recorded using a PerkinElmer Frontier spectrometer, with the background being measured under identical conditions (4000–500 cm^{-1}, 4 cm^{-1} resolution, and 64 scans) at room temperature. The spectra were ATR-corrected and baseline corrected.

2.8. Nuclear magnetic resonance (NMR) spectroscopy

^1H NMR spectra and ^7Li NMR of the samples were measured using a Bruker Avance III 500 MHz spectrometer at 60 °C. Samples were filled into flame-sealed 3 mm capillary tubes, which were then inserted into 5 mm NMR tubes filled with D_2O for field lock and the accurate referencing of chemical shifts of the samples. This setup was used to avoid the interaction of cobalt(II) and lithium(I) with D_2O, which would affect the accuracy of the experimental analysis.

2.9. Electrochemical measurements

Cyclic voltammetry (CV) experiments were performed with a VMP 300 multichannel potentiostat (Bio-logic, USA) at 60 °C after bubbling the leachate with N_2 gas for 30 minutes to displace O_2 in the solutions. N_2 gas flow was maintained just above the leachate during the experiment to minimise the oxygen content in the solutions.

The electrochemical experiments were performed with a conventional three-electrode setup using 1.6 mm diameter glassy carbon and 1.5 mm diameter Ni as the working electrodes (ALS Co. Ltd, Japan), 0.5 mm diameter platinum wire (XRF scientific) as the counter electrode (CE) and the Ag/Ag^+ reference electrode (RE) consisting of a Ag wire immersed in 5 mM AgOTf dissolved in CA : ChCl : H_2O (1 : 1 : 1), separated from the bulk solution by a porous frit. Prior to each experiment, the working electrode was polished with 0.3 μm alumina powder on a clean polishing cloth and cleaned by sonication in deionised water.

The electrode was dried in the oven at 70 °C for 10 minutes before placing in the experimental setup.

The reference electrodes were calibrated using ferrocene as an internal standard. The half wave potential for ferrocene in these systems was +0.324 V. The electrochemical experiments were performed at 60 °C at 50 mV s^{-1} scan rate, and a 1 mL solution mixture was used for each experiment. The water content of the solution mixtures was determined by Karl–Fischer (Metrohm, Switzerland) titration before and after the electrochemical experiments.

2.10. Scanning electron microscopy (SEM) and energy dispersive X-ray (EDX) spectroscopy

The samples were prepared by electrodeposition of cobalt onto a 4.5 mm diameter nickel foil (99.99%, Alfa-Aesar) for 45 min. Before electrodeposition experiments, Ni foil was etched with 1 M HCl, distilled water and isopropanol, followed by sonication in each chemical for 2 min to clean the surface. Then, the foils were dried at 100 °C in vacuum overnight and masked with Kapton tape, with exception of the 4.5 mm diameter circle. Cobalt electrodeposition was performed at −1.22 V *vs.* Fc/Fc^+ in the leachate from Co_3O_4.

The deposits were then rinsed with ethanol for 15 min to remove the excess electrolyte, and dried under vacuum for 10 min to remove ethanol. Samples were then mounted on an air-sensitive SEM sample holder. SEM measurements were performed using JSM-IT300 (JEOL Ltd, Japan) equipped with an Oxford x-max 50 mm^2 silicone drift detector at an acceleration voltage of 5 kV and 30 pA probe current. EDX mapping was performed at an acceleration voltage of 10 kV and at high current mode for 20 minutes.

3. Results and discussion

3.1 Role of additives in DES in the leaching of cobalt sources

Our study aims to gain a comprehensive understanding of the role of water as an additive in the cobalt leaching process, either just as a means to reduce the viscosity of DES or having an active role. First, Co_3O_4 was chosen as the optimum model compound to understand cobalt leaching without the impact from other metals generally present in secondary sources. Leaching of cobalt (II, III) oxide (Co_3O_4) using CA : ChCl (1 : 1) with 20 wt% of either water or ethylene glycol (EG) as an additive was performed in accordance with previous studies from the literature.[16] The leaching efficiency was similar when using either water (efficiency: 4.2%) or EG (efficiency: 3.2%). However, from those results (Table 2), it was clear that viscosity is not the only factor governing cobalt leaching, as the viscosity values differed by an order of magnitude (30 mPa s with water *vs.* 257 mPa s with EG). It is important to highlight that apart from the viscosity, the molar ratio of the two leaching solvents is also different (mole ratio CA : ChCl : H_2O = 1 : 1 : 4 *vs.* CA : ChCl : EG = 1 : 1 : 1.1). Thus, to investigate the impact of water in more detail, the leaching of Co_3O_4 using additives with the same molar ratio was carried out (Table 2). Fig. 1 presents the correlation between the cobalt leaching efficiencies and dynamic viscosities as a result of the chemical nature and amount of additives.

A decrease in water content from 4 to 1 molar ratio (20 wt% to 5.3 wt%), in relation to CA : ChCl (1 : 1), results in a decrease in the amount of cobalt(II) leached (by 2864 ppm) in CA : ChCl : H_2O (1 : 1 : 1), which is in agreement with an increase in viscosity (from 30 mPa s to 445 mPa s). Similar behaviour was observed when using EG as the additive, but only at lower concentrations from 1.1 to 0.3 molar ratio (20 wt% to 5.3 wt%). Thus, a decrease in the amount of cobalt(II) leached (by 801 ppm) is observed with an increase in viscosity from 257 mPa s to 1196 mPa s. However, upon adding larger amounts of EG up to a molar ratio of 4 (73 wt%), in relation to CA : ChCl (1 : 1), the leached cobalt(II) concentration is significantly decreased, leading to the lowest value in the series (by 1697 ppm). These findings indicate that EG could have another competing role in the leaching mechanism, and is not only limited to reducing the viscosity of the leaching solvent, as the viscosity in this specific case is much more favourable (41 mPa s, Table 2).

After considering the mole ratio of the components, EG is now in a much larger amount than CA, so we hypothesized that different complexation agents are competing to coordinate to cobalt(II). This solution (cobalt(II) in CA : ChCl : EG (1 : 1 : 4)) still showed a blue colour, similar to all other solutions in Table 2, demonstrating that the tetrahedral coordination geometry for cobalt(II) remains.[26]

3.2 FTIR analysis

Both CA and EG are strong chelating agents that can form complexes with metals, such as cobalt(II), in a known strategy for metal dissolution.[27–30] From the literature, it is known that CA and EG can coordinate to cobalt(II) in both mono- or bidentate symmetry, depending on the metal/ligand ratio and pH

Table 2 Cobalt leaching efficiency from Co_3O_4 using a series of leaching solvents at 60 °C for 72 h with a 1 : 5 solid-to-liquid (S:L) ratio, and the viscosity of the neat leaching solvent at 60 °C

Leaching solvents (DES + additive)				
Additives in CA : ChCl (1 : 1)	CA : ChCl: additive (molar ratio)	Leached Co(II) (ppm) solid to liquid (S : L) ratio 1 : 5	Co leaching efficiency %	Lovis dynamic viscosity of the neat leaching solvent/mPa s (Lovis variation coefficient)
CA : ChCl (1 : 1) + 5.3 wt% H_2O	1 : 1 : 1	4998 ± 359	2.6 ± 0.2	445 (0.9%)
CA : ChCl (1 : 1) + 5.3 wt% EG	1 : 1 : 0.3	5318 ± 343	2.7 ± 0.2	1196 (0.4%)
CA : ChCl (1 : 1) + 20 wt% H_2O	1 : 1 : 4	7862 ± 501	4.2 ± 0.3	30 (0.5%)
CA : ChCl (1 : 1) + 20 wt% EG	1 : 1 : 1.1	6119 ± 416	3.2 ± 0.2	257 (0.1%)
CA : ChCl (1 : 1) + 73 wt% EG	1 : 1 : 4	4422 ± 107	2.4 ± 0.1	41 (0.2%)

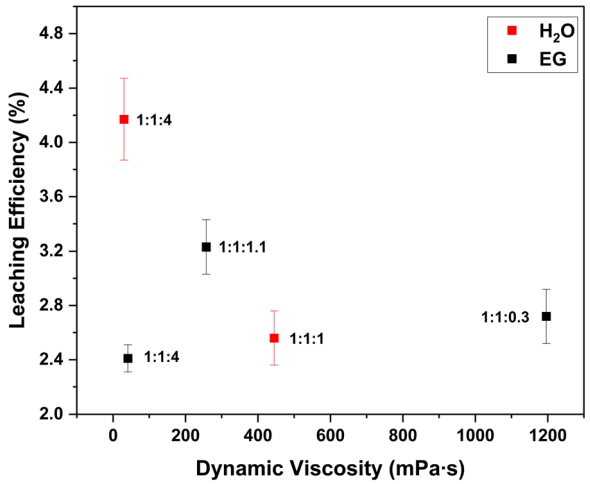

Fig. 1 Relationship of the cobalt leaching efficiency with dynamic viscosity upon varying the amount and type of additive (EG and water) added in the DES. Working temperature: 60 °C, solid : liquid (S : L) ratio: 1 : 5, time duration: 72 h, stirring rate: 700 rpm.

of the media.[31,32] Hence, FTIR spectroscopy was conducted to investigate in more detail the coordination environment of cobalt(II) in CA : ChCl : EG (1 : 1 : 4) and CA : ChCl : EG (1 : 1 : 1.1) to understand the large difference in the cobalt leaching efficiency between those two mixtures (Fig. 2(b–d)). For comparison, the neat compounds (CA, ChCl and EG) were analysed to identify the functional groups in these leaching solvents (Fig. 2(a)), and the band assignments are in the ESI.†

The cobalt-containing leachates with either CA : ChCl : EG 1 : 1 : 4 or 1 : 1 : 1.1 molar ratio were investigated (Fig. S1, ESI†), and no significant changes in the bands compared to the respective neat leaching solvent were observed. This could be due to the low concentration of cobalt(II) in the leachates in comparison with the amount of DES, which could overlap some of the cobalt-based bands. Therefore, cobalt(II) was significantly increased in the two neat leaching solvents to achieve approximately five times higher cobalt(II) concentration (0.5 mol L^{-1}) than in the leachates. Cobalt sulfate heptahydrate ($CoSO_4 \cdot 7H_2O$) salt was chosen instead of $CoCl_2 \cdot 6H_2O$ salt to prevent any possible alteration in the coordination environment of cobalt(II) due to its chlorophilic nature.[33]

Under those conditions, it is important to mention that in the CA : ChCl : EG (1 : 1 : 1.1) mixture, EG and CA are present in an approximately similar molar ratio with respect to cobalt(II) (Co(II) : EG = 1 : 7 and Co(II) : CA = 1 : 5.9). Conversely, in CA : ChCl : EG (1 : 1 : 4), EG is present in an approximately four times higher ratio than CA with respect to Co(II) (Co(II) : EG = 1 : 16.9

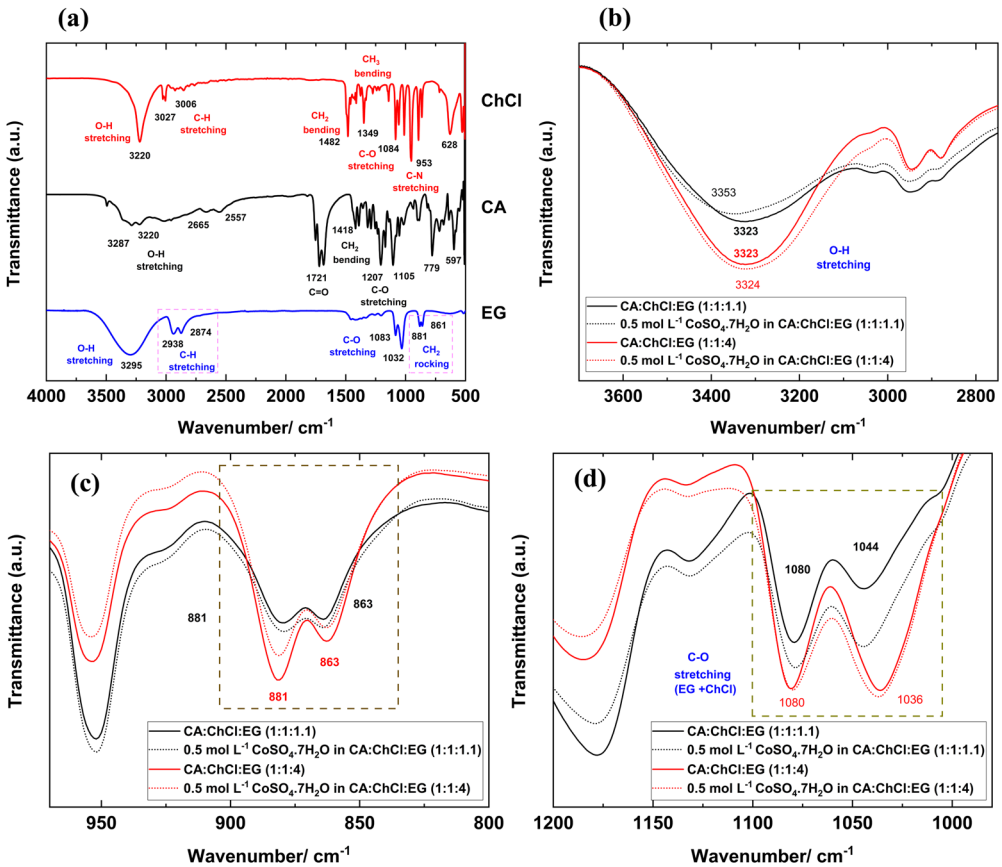

Fig. 2 (a) FTIR spectra of ethylene glycol (EG), citric acid (CA) and choline chloride (ChCl) analysed at room temperature. FTIR spectra of neat CA : ChCl : EG (1 : 1:1.1), neat CA : ChCl : EG (1 : 1 : 4), 0.5 mol L^{-1} $CoSO_4 \cdot 7H_2O$ in CA : ChCl : EG (1 : 1 : 1.1) and 0.5 mol L^{-1} $CoSO_4 \cdot 7H_2O$ in CA : ChCl : EG (1 : 1 : 4): (b) 3700–2750 cm^{-1} region, (c) 970–800 cm^{-1} region and (d) 1200–980 cm^{-1} region.

and Co(II) : CA = 1 : 4). The molar ratio of all the components presents in the two solutions relative to 1 cobalt(II) are summarized in Table S1 (ESI†).

A shift to a higher wavenumber (from 3323 cm^{-1} to 3353 cm^{-1}) was observed in the O–H stretching band when cobalt(II) was present in the CA : ChCl : EG (1 : 1 : 1.1) in comparison to the neat solvent system, whereas no shift was observed in the cobalt(II) containing CA : ChCl : EG (1 : 1 : 4) (Fig. 2(b)). It is difficult to draw conclusions on metal coordination from evaluation of the O–H stretching band region, as there is an overlap with the signal from water. However, it is important to note that the solution of cobalt(II) in CA : ChCl : EG (1 : 1 : 4) has a higher water content (<100 000 ppm) than the solution of cobalt(II) in CA : ChCl : EG (1 : 1 : 1.1) (<84 000 ppm), and yet no difference in the peak position of the O–H stretching band was observed in the former. The presence of OH groups in the three components (EG, CA and ChCl) makes it difficult to definitively identify the origin of the shift. However, there is no change observed in the C=O band of CA in the presence of cobalt(II), suggesting the coordination to EG as a much more likely reason than coordination to CA.

Additionally, Fig. 2(c) shows that the relative intensity for the CH_2 rocking vibration band corresponding to EG at 881 cm^{-1} (probably corresponding to bidentate coordination) is larger than the band at 863 cm^{-1} (corresponding to probable monodentate coordination) for CA : ChCl : EG (1 : 1 : 4) in the presence of cobalt(II).[32,34] In contrast, CA : ChCl : EG (1 : 1 : 1.1) shows similar intensity for both bands, showing a difference in the coordination manner (bidentate and monodentate ratio) of EG in the two solutions.[35]

Furthermore, Fig. 2(d) shows two C–O stretching bands; one at 1080 cm^{-1} observed in both CA : ChCl : EG (1 : 1 : 4) and CA : ChCl : EG (1 : 1 : 1.1), originating from EG and ChCl, and the other band originating only from EG at 1036 cm^{-1} in CA : ChCl : EG (1 : 1 : 4) and 1044 cm^{-1} in CA : ChCl : EG (1 : 1 : 1.1). The difference in the position of this band (1036 cm^{-1} *vs.* 1044 cm^{-1}) demonstrates the difference in the chemical environment of EG in the two neat leaching solvents. Nevertheless, the presence of Co(II) in CA : ChCl : EG (1 : 1 : 1.1) has increased the intensity of the 1044 cm^{-1} band to a greater extent compared to the 1080 cm^{-1} band, creating a relative intensity difference between the two C–O stretching peaks, indicating a likely coordination of cobalt(II) to EG.[36]

In summary, cobalt(II) coordinates to EG in two solutions in a different manner. EG presents different conformers based on its concentration in the neat DES composition. It is proposed that in CA : ChCl : EG (1 : 1 : 1.1), there is an equal contribution of mono- and bi-dentate coordination. Conversely, in CA : ChCl : EG (1 : 1 : 4), a bidentate coordination form of EG is more favourable. This difference may be responsible for the differences in the cobalt leaching efficiency.

After the in-depth study of the role of additives in the citric acid-based DES, CA : ChCl : EG in a 1 : 1 : 1.1 molar ratio was selected for further studies and optimisation based on its relatively high cobalt leaching efficiency (3.2%) and moderate viscosity (257 mPa s). In addition, our study aims to perform cobalt leaching, followed by electrodeposition of cobalt in the same pot. Therefore, having EG instead of water in the solution would be beneficial in enhancing the electrochemical window of the electrolyte.

3.3. Impact of other metals on the leaching of cobalt using CA : ChCl : EG (1 : 1 : 1.1) and experimental optimisation

To investigate the experimental time required, a Co_3O_4 leaching study was performed for 72 h at 60 °C using a stirring rate of 700 rpm and 1 : 5 S : L ratio to ensure consistency with the previous experiments. According to Fig. S2 (ESI†), no significant increase in the leaching efficiency after 48 h was observed. Therefore, the working time was limited to 48 h for the rest of the experiments.

Lithium cobalt oxide ($LiCoO_2$ or LCO) was chosen to continue with the cobalt leaching studies. This selection helped in limiting the number of variables since it only contains lithium apart from cobalt in the composition. The same experimental conditions for leaching were used as in the Co_3O_4 leaching (1 : 5 S : L ratio, temperature: 60 °C and 700 rpm stirring rate) in CA : ChCl : EG in (1 : 1 : 1.1), but for 48 h. In this study, measurements of lithium leaching were also conducted. According to the results obtained (Table 3), the cobalt solubility and leaching efficiency are higher (almost double) in LCO (8699 ppm and 5.6%) compared to that in Co_3O_4 (6119 ppm and 3.2%).

This significant difference in cobalt leaching could be due to several factors; namely, differences in the particle size, structure, and leaching mechanism. The particle size of the Co_3O_4 used in this study was <10 μm, and that for LCO was smaller (2–5 μm). Thus, the higher leaching efficiency may be due to the greater surface area.[37,38] In addition, LCO has a layered structure consisting of cobalt(III) (octahedral CoO_6^-) and lithium(I) in the interstitial spaces, whereas Co_3O_4 has a spinel structure consisting of cobalt(III) in octahedral sites and cobalt(II) in tetrahedral sites.[39–41] Zhao *et al.* reported that the depletion of lithium(I) eventually leads to a collapse in the crystal layered structure.[42] Hence, it could be assumed that the leaching of lithium(I) may weaken the LCO structure, facilitating the leaching of cobalt in comparison with Co_3O_4.

In our study, the lithium leaching efficiency (8.1%) was higher compared to the cobalt leaching efficiency. This is in agreement with the results from Gao *et al.*, which showed that the lithium leaching process is not controlled by any redox reaction, in contrast to the cobalt leaching process.[43]

Table 3 Cobalt and lithium leaching from $LiCoO_2$ using CAM : ChCl : EG (1 : 1 : 1.1) at 60 °C using 700 rpm stirring rate for different time durations and two different S : L ratios (1 : 5 and 1 : 66)

S : L ratio	Time (h)	Co solubility (ppm)	Co leaching efficiency %	Li solubility (ppm)	Li leaching efficiency %
1 : 5	48	8699 ± 162	5.6 ± 1	1487 ± 28	8.1 ± 1
1 : 66	4	1026 ± 56	8.5 ± 1	268 ± 15	18.9 ± 1
	24	2209 ± 37	18.3 ± 1	503 ± 8	35.4 ± 1
	48	5175 ± 301	43.0 ± 3	921 ± 54	65.2 ± 4
	72	4544 ± 437	38.0 ± 4	813 ± 78	57.0 ± 5

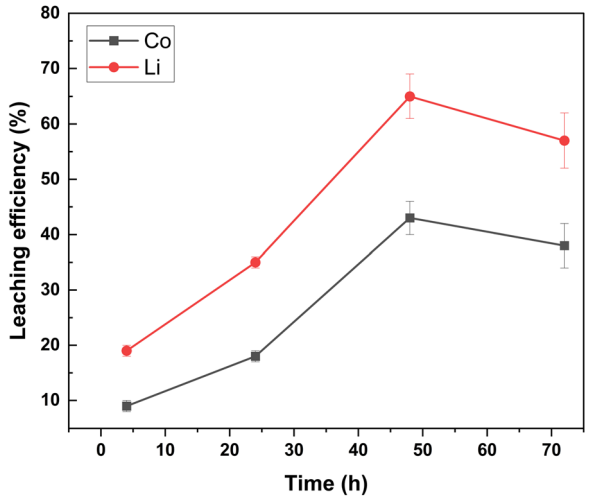

Fig. 3 Cobalt and lithium leaching efficiencies from $LiCoO_2$ using CA : ChCl : EG (1 : 1 : 1.1) at S : L ratio = 1 : 66, 700 rpm, 60 °C and different times.

Nevertheless, the leaching efficiencies in this work, for both cobalt and lithium, are low compared to state-of-the-art leaching materials, and this may be due to the high viscosity of the media.[16] Therefore, the amount of the leaching solvent was increased and adjusted to 1 : 66 (S : L ratio = 20 g L^{-1}) to reduce the system viscosity, and the media availability to leach metals. Under those conditions, we were able to accomplish higher leaching efficiencies (43.0% cobalt and 65.2% lithium) at 48 h (as shown in Fig. 3 and Table 3) from $LiCoO_2$ in comparison to the work of Peeters *et al.* (cobalt (~25%) and lithium (~50%)).[16] Peeters *et al.* performed a similar leaching experiment with $LiCoO_2$ in the absence of reducing agents, using CA : ChCl (1 : 2) + 35 wt% of water with the same S:L ratio as our experiments (20 g L^{-1}).[16] Thus, this enhancement could be due to the slightly higher working temperature (60 °C *vs.* 40 °C), higher amount of CA (50 mol% *vs.* 33 mol%) and the presence of EG. EG is a commonly used reducing agent for the synthesis of metallic nanoparticles and metal leaching, and its presence could be the main cause for this observed difference.[5,44]

3.4 Comparison of the electrochemical behaviour of leached cobalt(II) from Co_3O_4 and $LiCoO_2$

To realise the 'one-pot' approach, it is necessary to investigate the electrochemical behaviour of cobalt in the presence of other metal ions present after LIBs cathode leaching (*e.g.*, lithium(I)). Hence, the electrochemical behaviour of cobalt(II) in the leachates from Co_3O_4 and $LiCoO_2$ using CA : ChCl : EG (1 : 1 : 1.1) was investigated *via* cyclic voltammetry at 60 °C (Fig. 4).

The electrochemical stability of the leaching solvent (in the absence of cobalt(II)) was analysed prior to the leachates under the same working conditions. For that, the potential was scanned in positive and negative directions separately after polishing the WEs to ensure only the leaching solvent degradation was detected.

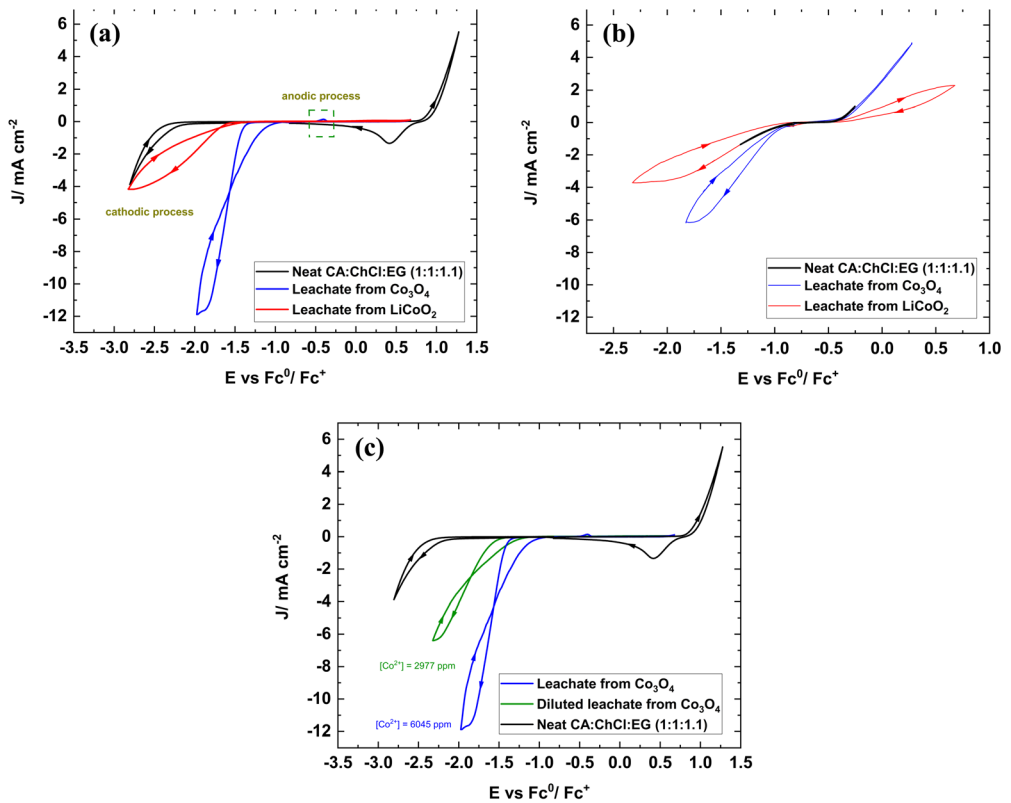

Fig. 4 Cyclic voltammograms corresponding to cobalt(II) in the leachates from Co_3O_4 and $LiCoO_2$ and the neat CA : ChCl : EG(1 : 1 : 1.1) using a (a) GC working electrode and (b) Ni working electrode and (c) comparison of the Co_3O_4 leachate with diluted Co_3O_4 leachate using the GC working electrode. Scan rate: 50 mV s^{-1} and temperature: 60 °C.

The electrochemical window lies from −2.40 V to 0.95 V *vs.* Fc/Fc^+ for glassy carbon (GC) as the working electrode (WE), whereas it is substantially narrower, −1.20 V to −0.26 V, for Ni WE probably due to its catalytic properties.[23,45]

Approximately similar concentrations (~0.1 mol L^{-1}) of the leachates from Co_3O_4 (6045 ppm) and $LiCoO_2$ (5543 ppm) were selected for the electrochemical comparison. The leachate from Co_3O_4 showed a higher cathodic peak current density (11.6 mA cm^{-2} on GC and 6.2 mA cm^{-2} on Ni), and a more positive cathodic onset (−1.41 V *vs.* Fc/Fc^+ on GC and −0.95 *vs.* Fc/Fc^+ on Ni) and peak potential (−1.87 V *vs.* Fc/Fc^+ on GC and −1.62 *vs.* Fc/Fc^+ on Ni) compared to the leachate from $LiCoO_2$ (Fig. 4a and b). All values are shown in Table 4.

The lower peak current density in the leachate from $LiCoO_2$ may be due to the slightly lower cobalt(II) concentration and/or different diffusion properties. The slope of the cathodic process is steeper for the leachate from Co_3O_4, reflecting a kinetic hindrance in the redox process of the leachate from $LiCoO_2$. These observations could be the result of the presence of lithium(I) (730 ppm) in the leachate, as well as the Co(II).

The reduction of cobalt(II) from both leachates on Ni WE was easier compared to GC WE. However, the cathodic peak and the decomposition of the solvent are too close for an efficient electrodeposition process (Fig. 4(b)). Another interesting observed phenomenon is that both leachates show an insignificant peak in the anodic process when using GC WE (Fig. 4(a)). The nature of this anodic peak could be either due to the oxidation of cobalt(II) to cobalt(III) or cobalt metal to cobalt(II), which is also known as cobalt stripping. To investigate this, the potential was scanned only in the positive direction in both cases (*i.e.*, without cobalt deposition first). No peaks were observed, as shown in Fig. S3 (ESI†) (insets), proving that the anodic process corresponds to the cobalt stripping.

To investigate the difference in the current density of the cathodic peaks, the leachate from the Co_3O_4 was diluted approximately by half by adding the neat leaching solvent, CA : ChCl : EG (1 : 1 : 1.1) until the concentration of cobalt(II) was 2977 ppm. Even though the concentration of cobalt(II) is lower than the leachate from $LiCoO_2$, it still shows a higher cathodic current density, more positive cathodic onset and peak potential, showing that cobalt(II) concentration is not the main factor that governs the current density (Fig. 4(c), using GC WE). Since the temperature, scan rate and WE that were used are similar in both cases, the physicochemical properties (*e.g.*, viscosity and ionic conductivity) of the two leachates were investigated in more detail to determine if these may be the reason for the different current densities.

The viscosity of the leachate from $LiCoO_2$ is higher (by 550 mPa s) and the conductivity is slightly lower (by 0.19 mS cm^{-1}) in comparison with leachate from Co_3O_4, thereby demonstrating that the inferior mass transport properties could be a possible reason for its lower cathodic current density.

3.5 Investigation of cobalt(II) speciation in the two leachates

Both leachates, using $LiCoO_2$ and Co_3O_4 as the source, are blue in colour, demonstrating the presence of tetrahedrally coordinated cobalt(II) as the dominant species.[46,47] Even though $CoCl_4^{2-}$ is the mostly reported tetrahedral geometry for cobalt(II) in Cl^--containing media, mixed ligand environments demonstrating a tetrahedral geometry have also been reported in the literature.[48,49] We hypothesise that the nature of the ligands that are coordinated to cobalt(II) is different in the two leachates (in the presence and absence of lithium(I)) since it led to a significant difference in the cobalt(II) reduction potentials.

^{59}Co NMR is not suitable for direct measurement of cobalt(II) speciation due to its paramagnetic nature, with very rapid nuclear relaxation rates.[50] However, the magnetic properties of other nuclei in the same sample are affected by the presence of paramagnetic species, hence NMR of other nuclei could reveal information regarding the coordination environment of cobalt(II).[50] Therefore, ^1H NMR and ^7Li NMR analyses were conducted at 60 °C, which is the same temperature as the electrochemical experiments, to investigate the speciation of cobalt(II) in the two leachates.

All the peaks for ^1H NMR analysis of CA, ChCl and EG are assigned and labelled in Fig. 5(a), and the chemical shift values are provided in the ESI.† Fig. 5(b) shows the ^1H NMR of CA : ChCl : EG (1 : 1 : 1.1), and the two leachates from Co_3O_4 and $LiCoO_2$. In general, broadening of the peaks and shifts to high ppm values (deshielding) were observed, indicating the presence of a paramagnetic complex in the two leachates compared to the neat CA : ChCl : EG (1 : 1 : 1.1).[51–53] All the protons corresponding to the hydroxyl groups (*e.g.*, carboxylic protons of CA and hydroxyl protons of EG and ChCl) appear as one broad band, labelled as "z" in CA : ChCl : EG (1 : 1 : 1.1) (based on the integration).

Between the two leachates, the leachate from Co_3O_4 shows a higher extent of paramagnetic shift in the protons from the neat CA : ChCl : EG (1 : 1 : 1.1), suggesting a shorter average distance to the paramagnetic center (cobalt(II)). Furthermore, a larger shift to high ppm values (by 4.40 ppm *vs.* 3.47 ppm) was

Table 4 Cathodic peak current density, cathodic peak potential using GC and Ni as the WEs, water content, dynamic viscosity, and conductivity for the leachates from Co_3O_4 and $LiCoO_2$

Leachate		Cathodic peak current density (mA cm^{-2})	Cathodic peak potential (V)	Cathodic onset potential (V)	Water content (ppm)	Dynamic viscosity/mPa s (variation coefficient)	Conductivity/mS cm^{-1} (standard deviation)
From Co_3O_4	GC WE	11.6	−1.87	−1.41	<64 000	297 (0.74%)	1.46 (± 0.004)
	Ni WE	6.2	−1.62	−0.95			
From $LiCoO_2$	GC WE	4.0	−2.63	−1.64	<61 000	847 (0.33%)	1.27 (± 0.015)
	Ni WE	3.7	−1.87	−1.01			

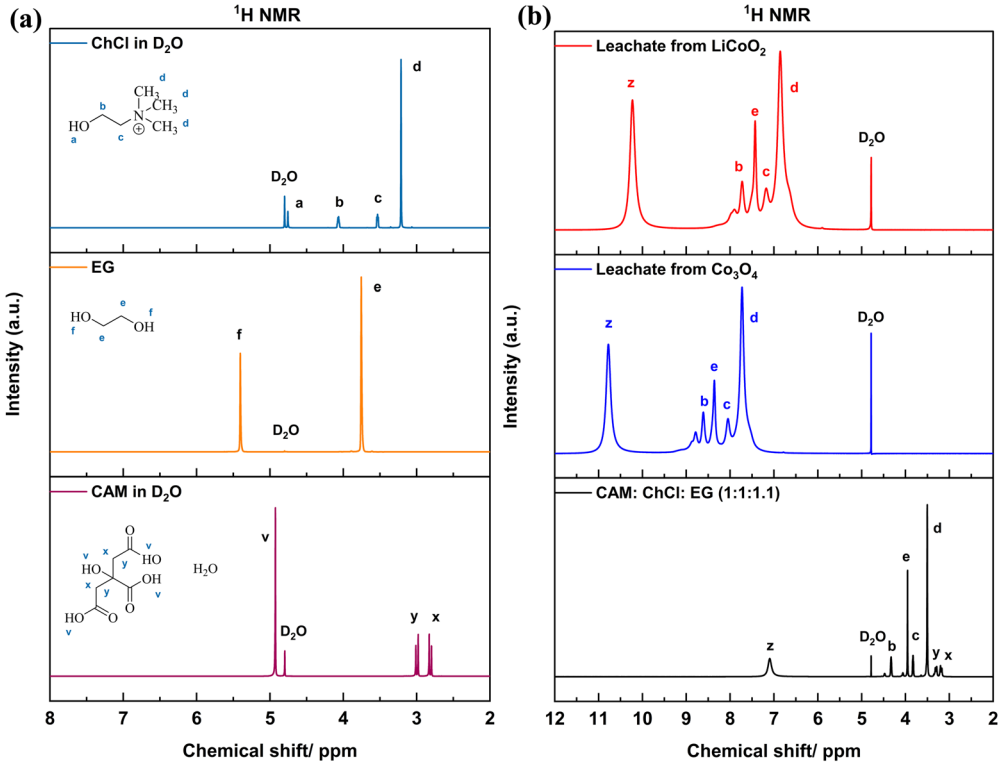

Fig. 5 (a) ^{1}H NMR spectra of ChCl dissolved in D_2O (top), EG (middle), and CA dissolved in D_2O (bottom) at 60 °C. (b) ^{1}H NMR spectra of CA : ChCl : EG (1 : 1 : 1.1) (bottom), leachate from Co_3O_4 (middle) and the leachate from $LiCoO_2$ (top) analysed at 60 °C.

observed for the aliphatic protons (e) of EG in the leachate from Co_3O_4 compared to $LiCoO_2$, indicating a probable coordination of cobalt(II) to EG, which is in agreement with the FTIR analysis. The peaks from the aliphatic protons from CA (*x* and *y*) also merged with those (d) of ChCl in both leachates. The leachate from Co_3O_4 shows a large shift to high ppm values (approximately by 4.30 ppm *vs.* 3.40 ppm), which also suggests coordination of cobalt(II) to CA. All the chemical shift values of protons in CA : ChCl : EG (1 : 1 : 1.1) and the two leachates from Co_3O_4 and $LiCoO_2$ are given in Table 5.

Considering that both leachates contain approximately similar cobalt(II) concentrations, the presence of lithium(I) in the leachate from $LiCoO_2$ is the major difference between the two leachates. This indicates that the presence of lithium(I) in the leachate most likely plays a role in limiting cobalt(II) coordination to the solvent system. To investigate in detail the role of lithium(I), a control sample with a similar concentration of lithium(I) was prepared by dissolving lithium bromide (LiBr) in CA : ChCl : EG (1 : 1 : 1.1) and analysed with both ^{1}H (Fig. 6a) and ^{7}Li NMR (Fig. 6b). This experiment aimed to explore the coordination of lithium(I) in the CA : ChCl : EG (1 : 1 : 1.1) in the absence of cobalt. LiBr was selected instead of LiCl to maintain a probable coordination ligand (*e.g.*, Cl^-) concentration constant in the control sample. The ^{1}H NMR spectra using LiBr presented a slight shift to lower ppm value (by 0.04 ppm) of the peak corresponding to "z" protons for the LiBr solution compared to CA : ChCl : EG (1 : 1 : 1.1) (Fig. 6a). Thus, lithium(I) is likely to form coordination complexes with both CA and EG, owing to the coordinating abilities of these ligands.

Both ^{7}Li NMR spectra showed one peak, but different chemical environments of lithium(I) in the leachate from $LiCoO_2$ and the control sample (LiBr in the CA : ChCl : EG (1 : 1 : 1.1) (Fig. 6b). The peak from the $LiCoO_2$ leachate exists at high ppm compared to the peak from the control sample

Table 5 Chemical shift values of protons in CA : ChCl : EG (1 : 1 : 1.1), leachate from Co_3O_4 and leachate from $LiCoO_2$. The extent of the paramagnetic shift with respect to CA : ChCl : EG (1 : 1 : 1.1) for the leachates are given in brackets

Proton label	Chemical shifts in CA : ChCl : EG (1 : 1 : 1.1) (ppm)	Chemical shifts (ppm) in the leachate from Co_3O_4 (size of paramagnetic shift)	Chemical shifts (ppm) in the leachate from $LiCoO_2$ (size of paramagnetic shift)
z[a](a + f + v)	7.10	10.77 (by 3.67)	10.22 (by 3.13)
b	4.32	8.61 (by 4.29)	7.72 (by 3.40)
e	3.95	8.35 (by 4.40)	7.42 (by 3.47)
c	3.82	8.04 (by 4.22)	7.17 (by 3.35)
d	3.50	7.72 (by 4.22)	6.85 (by 3.35)

[a] From the integration data.

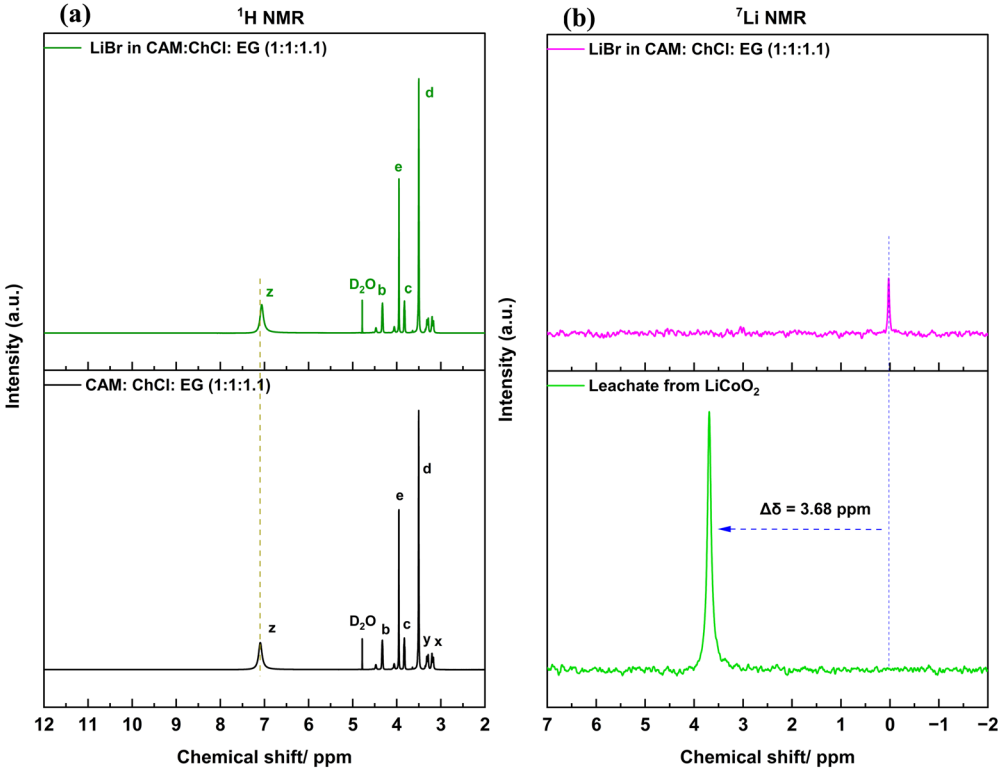

Fig. 6 (a) ^{1}H NMR spectra of CA : ChCl : EG (1 : 1 : 1.1) and LiBr dissolved in CA : ChCl : EG (1 : 1 : 1.1) analysed at 60 °C and (b) ^{7}Li NMR spectra of LiBr dissolved in CA : ChCl : EG (1 : 1 : 1.1) and the leachate from $LiCoO_2$ analysed at 60 °C.

(by 3.68 ppm), demonstrating a paramagnetic influence due to the lower distance to cobalt(II). In addition, a slight broadening was observed in the peak from $LiCoO_2$ leachate compared to the peak from the LiBr, further corroborating the paramagnetic influence.

In summary, it is proposed that lithium(I) coordination to EG and/or CA in the leaching solvent has limited the coordination of those ligands to cobalt(II) in the leachate from $LiCoO_2$, which led to the difference in the cobalt(II) reduction potentials.

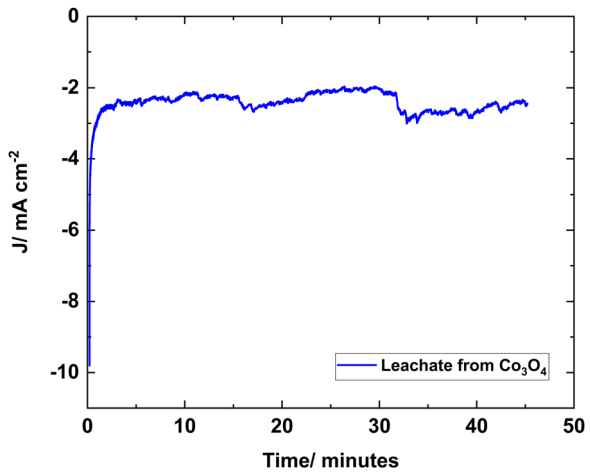

Fig. 7 Chronoamperometric response corresponding to the leachate from Co_3O_4 on an Ni foil. Deposition time: 45 minutes at 60 °C.

3.6 Electrodeposition of cobalt

Nickel working electrodes have been effectively employed previously for metal electrodeposition,[54,55] including cobalt,[56] whereas GC has been reported as a difficult substrate for metal electrodeposition.[57] Hence, potentiostatic deposition was carried out on nickel foil in Co_3O_4 leachate for 45 minutes at 60 °C, using a citric acid-based DES for the first time as a proof of concept (Fig. 7).

Electrodeposition was not performed with the $LiCoO_2$ leachate. This is because the cathodic process is too close to the neat solvent degradation (Fig. 4b), impacting the efficiency and the purity of the electrodeposit. A mid potential value between the cathodic onset and peak potentials, according to Fig. 4(b), was chosen as the applied potential (−1.22 V *vs.* Fc/Fc^{+}) and repeated for reproducibility.

The chronoamperogram showed a noisy yet reasonably stable current density after the initial current spike, followed by a decay in the current. This spike and the decay in the current is due to the double layer charging at the applied potential, which is typical for metal electrodeposition, and the subsequent nucleation and growth of the metal on the substrate.[58] The noise could be due to the gas evolution, which was observed on the working electrode during the process, and the gas is most likely H_2 due the large amount of water (<64 000 ppm) present in the leachate. The leachates were used without drying after the leaching step to mimic the industrial electroplating conditions.

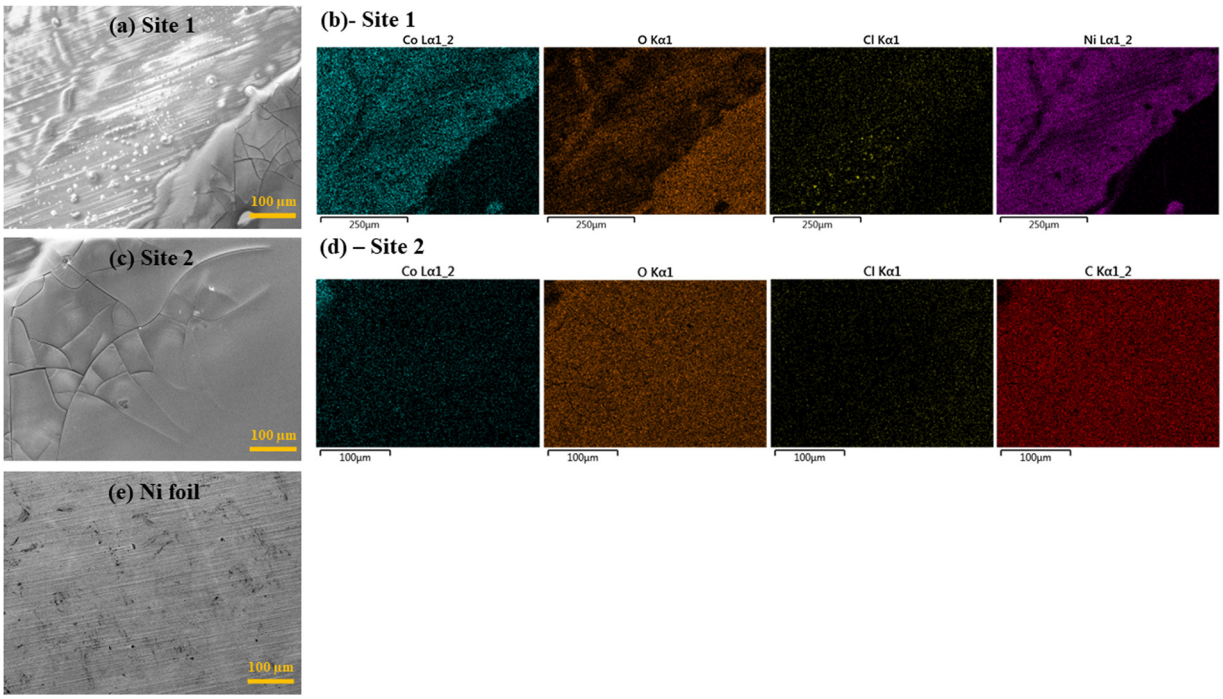

Fig. 8 (a) and (c) SEM images and (b) and (d) EDX mappings of the electrodeposit resulting from the Co_3O_4 leachate. (e) SEM image of Ni foil as the substrate.

The cathodic current efficiency was 33%, calculated assuming that all of the deposit is cobalt metal. This value is low compared to our previous studies (>78%) for cobalt deposition on Nickel foil using EG : ChCl (4.5 : 1) systems.[56] The difference could be due to the difference in the water contents, applied potential, the composition and the electrochemical stability of the DES.

The electrodeposit was characterised using SEM and EDX to investigate the surface morphology and the atomic composition, respectively, after washing the sample with ethanol for 15 minutes and drying under vacuum. Fig. 8 presents the surface morphology (Fig. 8a and c), showing two different sites (sites 1 and 2) of the electrodeposit.

A thin non-uniform layer in the inner masking area and a dense and continuous layer on the edge of the masking circular area were attained in the electrodeposition process (Fig. 8a), which was confirmed by repeating the experiment. This uneven distribution in the electrodeposit is most likely due to a larger current density on the edges of the masked circular electrodes.[59] EDX mapping and map spectra (Fig. 8b and Fig. S4(a), ESI†) show the presence of cobalt, chloride, oxygen in site 1, which mainly consists of the thin layer. The presence of nickel could be a result of the substrate, and also could be due to the overlapping of energy windows with those of cobalt $L\alpha_{1,2}$.[60] Oxygen may have originated from the water in the leachate, and may also be present due to the atmospheric exposure as the experiments are conducted and washed in air.[61,62] The dense area (site 2) (Fig. 8d and Fig. S4(b), ESI†) was composed of cobalt, chloride, oxygen and carbon. Carbon and chloride likely result from the decomposition of the solvent system. This shows that the electrodeposit obtained from the Co_3O_4 leachate does not contain only metallic cobalt. The atomic percentages of all the elements present in the electrodeposit (site 1 and 2) are shown in Table 6. The EDX map spectra of nickel foil (Fig. S4(c), ESI†) showed the presence of only nickel (96.6 at%) and oxygen (3.4 at%).

Table 6 Atomic percentages of elements present in the electrodeposit resulting from the Co_3O_4 leachate using CA : ChCl : EG (1 : 1 : 1.1)

	Co at%	O at%	Cl at%	C at%	Ni at%
Spectrum 1 Fig. S3(a) (ESI) – site 1	1.4	47.2	1.7	—	49.7
Spectrum 2 Fig. S3(b) (ESI) – site 2	0.9	42.5	0.6	55.9	—

4. Conclusion

This study investigated the role of additives in the cobalt leaching using a citric acid-based deep eutectic solvent (DES) under mild conditions, and shows the importance of the chemical nature and the concentration of additive in the leaching process. Different factors are considered when selecting additives, such as the boiling point or the presence of free protons. The findings indicate that while the addition of ethylene glycol (EG) as an additive reduces the overall viscosity of the media, it does not directly impact the leaching efficiency of cobalt. In contrast, the addition of water as an additive increased the leaching efficiency of cobalt.

FTIR spectroscopy analysis suggests different coordination of cobalt(II) with EG (CA : ChCl : EG in 1 : 1 : 1.1) in the leaching solvent compared to the leaching solvent with higher EG concentration (CA : ChCl : EG in 1 : 1 : 4), indicating a likely explanation for the observed variations in the cobalt leaching efficiency.

Moreover, the cobalt source (lithium cobalt oxide ($LiCoO_2$) or cobalt (II, III) oxide (Co_3O_4)) also plays a role in the leaching efficiency. This study succeeded in leaching 43% of cobalt and 65% of lithium from $LiCoO_2$ using CA : ChCl : EG (1 : 1 : 1.1) at 60 °C for 48 h in the absence of reducing agents, which is higher compared to the previous literature. This improved leaching is believed to result from the presence of EG in the leaching solvent, higher experimental temperature (60 °C) or an increase in the CA content.

Additionally, significant differences in the electrochemical behaviour of cobalt(II) was observed depending on the leachates. A more positive cathodic onset and peak potential was observed for Co_3O_4 compared to $LiCoO_2$ irrespective of the type of the WE. Therefore, it appears that lithium is beneficial during the cobalt leaching process, and is potentially influenced by the cobalt source, yet exhibits detrimental effects during cobalt electrodeposition.

^{1}H NMR studies showed a higher coordination of EG and CA to cobalt(II) in the absence of lithium(I) compared to its presence in the leachate, which is consistent with a difference in the cobalt(II) speciation between the two leachates.

Finally, as a proof of concept, a preliminary study of the electrodeposition of cobalt from Co_3O_4 leachate was carried out on nickel foil based on the favourability towards cobalt(II) reduction in CA : ChCl : EG (1 : 1 : 1.1). SEM images showed a non-uniform electrodeposit, and EDX elemental analysis displayed the presence of cobalt (1.4 at%) with chlorine, carbon, oxygen in the electrodeposit. This is the first time a one-pot system has being studied in citric acid-based DESs, and further studies are necessary towards achieving optimum efficiency and purity of the electrodeposits.

These insights on the influence of additives on cobalt leaching, and the effect of lithium(I) in the leachate on the electrochemical behaviour and speciation of cobalt(II), may be applied to design a sustainable electrochemical recovery process using DESs under mild conditions.

Data availability

The data supporting this article are available from the corresponding author on request.

Conflicts of interest

There are no conflicts to declare.

Acknowledgements

This research was supported by the Australian Research Council Training Centre for Future Energy Storage Technologies (grant agreement No IC180100049) and funded by the Australian Government. I. N. Perera acknowledges the financial support from Deakin University (DUPR Scholarship). C.P.G. gratefully acknowledges the financial support from EU (IONBIKE 2.0 MSCA-SE, grant agreement No 101129945).

References

1 K. K. Jena, A. AlFantazi and A. T. Mayyas, Comprehensive Review on Concept and Recycling Evolution of Lithium-Ion Batteries (LIBs), *Energy Fuels*, 2021, **35**(22), 18257–18284.
2 V. Chaudhary, P. Lakhera, K.-H. Kim, A. Deep and P. Kumar, Insights into the Eco-Friendly Recovery Process for Valuable Metals from Waste Lithium-ion Batteries by Organic Acids Leaching, *Sep. Purif. Rev.*, 2023, 1–18.
3 R. Golmohammadzadeh, F. Faraji, B. Jong, C. Pozo-Gonzalo and P. C. Banerjee, Current challenges and future opportunities toward recycling of spent lithium-ion batteries, *Renewable Sustainable Energy Rev.*, 2022, 159.
4 X. Zheng, Z. Zhu, X. Lin, Y. Zhang, Y. He, H. Cao, Z. Sun and A. Mini-Review, on Metal Recycling from Spent Lithium Ion Batteries, *Engineering*, 2018, **4**(3), 361–370.
5 M. K. Tran, M.-T. F. Rodrigues, K. Kato, G. Babu and P. M. Ajayan, Deep eutectic solvents for cathode recycling of Li-ion batteries, *Nat. Energy*, 2019, **4**(4), 339–345.
6 A. Chagnes and B. Pospiech, A brief review on hydrometallurgical technologies for recycling spent lithium-ion batteries, *J. Chem. Technol. Biotechnol.*, 2013, **88**(7), 1191–1199.
7 M. K. Jha, A. Kumari, A. K. Jha, V. Kumar, J. Hait and B. D. Pandey, Recovery of lithium and cobalt from waste lithium ion batteries of mobile phone, *Waste Manage.*, 2013, **33**(9), 1890–1897.
8 E. G. Pinna, M. C. Ruiz, M. W. Ojeda and M. H. Rodriguez, Cathodes of spent Li-ion batteries: Dissolution with phosphoric acid and recovery of lithium and cobalt from leach liquors, *Hydrometallurgy*, 2017, **167**, 66–71.
9 C. K. Lee and K. Rheeb, Reductive leaching of cathodic active materials from lithium ion battery wastes, *Hydrometallurgy*, 2003, **68**, 5–10.
10 L. Chen, X. Tang, Y. Zhang, L. Li, Z. Zeng and Y. Zhang, Process for the recovery of cobalt oxalate from spent lithium-ion batteries, *Hydrometallurgy*, 2011, **108**(1–2), 80–86.
11 C. Padwal, H. D. Pham, S. Jadhav, T. T. Do, J. Nerkar, L. T. M. Hoang, A. Kumar Nanjundan, S. G. Mundree and D. P. Dubal, Deep Eutectic Solvents: Green Approach for Cathode Recycling of Li-Ion Batteries, *Adv. Energy Sustainability Res.*, 2021, **3**, 1.
12 H. Li, N. Chen, W. Liu, H. Feng, J. Su, D. Fu, X. Liu, M. Qiu and L. Wang, A reusable deep eutectic solvent for the regeneration of Li and Co metals from spent lithium-ion batteries, *J. Alloys Compd.*, 2023, **966**, 171517.
13 Z. Yuan, H. Liu, W. F. Yong, Q. She and J. Esteban, Status and advances of deep eutectic solvents for metal separation and recovery, *Green Chem.*, 2022, **24**(5), 1895–1929.
14 E. Bağda, H. Altundağ, M. Tüzen, M. Soylak and A. Novel, Selective Deep Eutectic Solvent Extraction Method for Versatile Determination of Copper in Sediment Samples by ICP-OES, *Bull. Environ. Contam. Toxicol.*, 2017, **99**(2), 264–269.
15 E. Bağda, H. Altundağ and M. Soylak, Highly Simple Deep Eutectic Solvent Extraction of Manganese in Vegetable Samples Prior to Its ICP-OES Analysis, *Biol. Trace Elem. Res.*, 2017, **179**(2), 334–339.

16 N. Peeters, K. Binnemans and S. Riaño, Solvometallurgical recovery of cobalt from lithium-ion battery cathode materials using deep-eutectic solvents, *Green Chem.*, 2020, **22**(13), 4210–4221.
17 Y. Hua, Y. Sun, F. Yan, S. Wang, Z. Xu, B. Zhao and Z. Zhang, Ionization potential-based design of deep eutectic solvent for recycling of spent lithium ion batteries, *Chem. Eng. J.*, 2022, 436.
18 O. S. Hammond, D. T. Bowron, A. J. Jackson, T. Arnold, A. Sanchez-Fernandez, N. Tsapatsaris, V. Garcia Sakai and K. J. Edler, Resilience of Malic Acid Natural Deep Eutectic Solvent Nanostructure to Solidification and Hydration. The, *J. Phys. Chem. B*, 2017, **121**(31), 7473–7483.
19 O. S. Hammond, D. T. Bowron and K. J. Edler, The Effect of Water upon Deep Eutectic Solvent Nanostructure: An Unusual Transition from Ionic Mixture to Aqueous Solution, *Angew. Chem., Int. Ed.*, 2017, **56**(33), 9782–9785.
20 J. Robson, S. Townsend, P. Bowdler and K. C. Honeychurch, Direct thermal desorption gas chromatographic determination of toxicologically relevant concentrations of ethylene glycol in whole blood, *Analyst*, 2018, **143**(4), 963–969.
21 J. Fowles, M. Banton, J. Klapacz and H. Shen, A toxicological review of the ethylene glycol series: Commonalities and differences in toxicity and modes of action, *Toxicol. Lett.*, 2017, **278**, 66–83.
22 L. Chen, X. Tang, Y. Zhang, L. Li, Z. Zeng and Y. Zhang, Process for the recovery of cobalt oxalate from spent lithium-ion batteries, *Hydrometallurgy*, 2011, **108**(1), 80–86.
23 K. Periyapperuma, J. M. Pringle, L. Sanchez-Cupido, M. Forsyth and C. Pozo-Gonzalo, Fluorine-free ionic liquid electrolytes for sustainable neodymium recovery using an electrochemical approach, *Green Chem.*, 2021, **23**(9), 3410–3419.
24 S. Wang, Z. Zhang, Z. Lu and Z. Xu, A novel method for screening deep eutectic solvent to recycle the cathode of Li-ion batteries, *Green Chem.*, 2020, **22**(14), 4473–4482.
25 J. Liu, T. Y. Mak, Z. Meng, X. Wang, Y. Cao, Z. Lu, D. W.-S. Suen, X.-Y. Lu and Y. Tang, Efficient recovery of lithium as Li2CO3 and cobalt as Co3O4 from spent lithium-ion batteries after leaching with p-toluene sulfonic acid, *Hydrometallurgy*, 2023, 216.
26 R. Chueachot and R. Nakhowong, Synthesis and optical properties of blue pigment CoAl2O4 nanofibers by electrospinning, *Mater. Lett.*, 2020, **259**, 126904.
27 R. Golmohammadzadeh, F. Faraji and F. Rashchi, Recovery of lithium and cobalt from spent lithium ion batteries (LIBs) using organic acids as leaching reagents: A review, *Resour., Conserv. Recycl.*, 2018, **136**, 418–435.
28 A. Zhu, X. Bian, W. Han, D. Cao, Y. Wen, K. Zhu and S. Wang, The application of deep eutectic solvents in lithium-ion battery recycling: A comprehensive review, *Resour., Conserv. Recycl.*, 2023, 188.
29 S. Mishra, A. Pandey, K. K. Pant and B. Mishra, Investigating the effect of mono di carboxylic acids as hydrogen bond donor on solvation of copper in choline chloride-based deep eutectic solvents, *J. Mol. Liq.*, 2023, **383**, 122142.
30 A. P. Abbott, J. Collins, I. Dalrymple, R. C. Harris, R. Mistry, F. Qiu, J. Scheirer and W. R. Wise, Processing of Electric Arc Furnace Dust using Deep Eutectic Solvents, *Aust. J. Chem.*, 2009, **62**(4), 341–347.
31 Z.-H. Zhou, Y.-F. Deng and H.-L. Wan, Structural Diversities of Cobalt(II) Coordination Polymers with Citric Acid, *Cryst. Growth Des.*, 2005, **5**(3), 1109–1117.
32 D. Knetsch and W. L. Groeneveld, Alcohol as ligands. III. Complexes of Ethylene glycol with some divalent metal halides, *Inorg. Chim. Acta*, 1973, **7**, 81–87.
33 H. Bastos, N. Schaeffer, J. M. Pringle, J. A. P. Coutinho and C. Pozo-Gonzalo, Enhanced Dissolution of Metal Oxides in Hydroxylated Solvents - Towards Application in Lithium-Ion Battery Leaching, *ChemSusChem*, 2023, e202300455.
34 M. Akihisa, Infrared Spectra of Glycols Coordinated to Metal Ions, *Bull. Chem. Soc. Jpn.*, 1959, **32**(12), 1381–1383.
35 Y. Kuroda and M. Kubo, CH2 rocking vibrations of polyethylene glycols, *J. Polym. Sci.*, 1957, **26**(114), 323–328.
36 A. Ahmed and H. A. Tajmir-Riahi, Interaction of toxic metal ions Cd^{2+}, Hg^{2+}, and Pb^{2+} with light-harvesting proteins of chloroplast thylakoid membranes. An FTIR spectroscopic study, *J. Inorg. Biochem.*, 1993, **50**(4), 235–243.
37 Z. Ruan, M. Li, K. Gao, D. Zhang, L. Huang, W. Xu and X. Liu, Effect of Particle Size Refinement on the Leaching Behavior of Mixed Rare-Earth Concentrate Using Hydrochloric Acid, *ACS Omega*, 2019, **4**(6), 9813–9822.
38 S. Sahu and N. Devi, Two-step leaching of spent lithium-ion batteries and effective regeneration of critical metals and graphitic carbon employing hexuronic acid, *RSC Adv.*, 2023, **13**(11), 7193–7205.
39 K. Forster-Tonigold, J. Kim, J. Bansmann, A. Groß and F. Buchner, Model Studies on the Formation of the Solid Electrolyte Interphase: Reaction of Li with Ultrathin Adsorbed Ionic-Liquid Films and Co3O4(111) Thin Films, *Chem. Phys. Chem.*, 2021, **22**(5), 441–454.
40 S. Tang, M. Zhang, M. Guo and A. Novel Deep-Eutectic, Solvent with Strong Coordination Ability and Low Viscosity for Efficient Extraction of Valuable Metals from Spent Lithium-Ion Batteries, *ACS Sustainable Chem. Eng.*, 2022, **10**(2), 975–985.
41 C. Heubner, B. Matthey, T. Lein, F. Wolke, T. Liebmann, C. Lämmel, M. Schneider, M. Herrmann and A. Michaelis, Insights into the electrochemical Li/Na-exchange in layered $LiCoO_2$ cathode material, *Energy Storage Mater.*, 2020, **27**, 377–386.
42 S. Zhao, W. Zhang, G. Li, H. Zhu, J. Huang and W. He, Ultrasonic renovating and coating modifying spent lithium cobalt oxide from the cathode for the recovery and sustainable utilization of lithium-ion battery, *J. Cleaner Prod.*, 2020, **257**, 120510.
43 W. Gao, J. Song, H. Cao, X. Lin, X. Zhang, X. Zheng, Y. Zhang and Z. Sun, Selective recovery of valuable metals from spent lithium-ion batteries – Process development and kinetics evaluation, *J. Cleaner Prod.*, 2018, **178**, 833–845.
44 Y. Luo, L. Ou and C. Yin, A green and efficient combination process for recycling spent lithium-ion batteries, *J. Cleaner Prod.*, 2023, 396.
45 L. J. Small, J. M. Sears, T. N. Lambert, T. J. Boyle and R. F. Hess, Electroreduction of Er^{3+} in nonaqueous solvents, *RSC Adv.*, 2016, **6**(92), 89564–89571.

46 A. Y. M. Al-Murshedi, A. Al-Yasari, H. F. Alesary and H. K. Ismail, Electrochemical fabrication of cobalt films in a choline chloride–ethylene glycol deep eutectic solvent containing water, *Chem. Pap.*, 2019, **74**(2), 699–709.
47 B. A. Duell, J. Li and M. A. Subramanian, Hibonite Blue: A New Class of Intense Inorganic Blue Colorants, *ACS Omega*, 2019, **4**(26), 22114–22118.
48 R. Fukui, Y. Katayama and T. Miura, The effect of organic additives in electrodeposition of Co from an amide-type ionic liquid, *Electrochim. Acta*, 2011, **56**(3), 1190–1196.
49 S. Schaltin, P. Nockemann, B. Thijs, K. Binnemans and J. Fransaer, Influence of the Anion on the Electrodeposition of Cobalt from Imidazolium Ionic Liquids, *Electrochem. Solid-State Lett.*, 2007, **10**(10), D104–D107.
50 J. P. Allen, C. A. O'Keefe and C. P. Grey, Quantifying Dissolved Transition Metals in Battery Electrolyte Solutions with NMR Paramagnetic Relaxation Enhancement, *J. Phys. Chem. C*, 2023, **127**(20), 9509–9521.
51 R. J. Abraham, I. Marsden and L. Xiujing, NMR spectra of the porphyrins. Part 39. Paramagnetic shifts in cobalt(II) porphyrins, *Magn. Reson. Chem.*, 1990, **28**(12), 1051–1057.
52 E. N. Zapolotsky, S. P. Babailov and G. A. Kostin, Paramagnetic Properties and Moderately RapidConformational Dynamics in the Cobalt(II) Calix[4]arene Complex by NMR, *Molecules*, 2022, **27**, 14.
53 V. K. Voronov, I. A. Ushakov and E. A. Funtikova, The heterospin cobalt complexes: peculiarities of high-resolution NMR spectra, *Heliyon*, 2022, **8**(4), e09202.
54 Y. Jia, H. Cheng, J. Qiu, F. Han, Y. Zou, Z. Li, X. Zhou and H. Xu, Effect of temperature on diffusion behavior of Te into nickel, *J. Nucl. Mater.*, 2013, **441**(1–3), 372–379.
55 Y.-T. Huang, S.-P. Feng and C.-M. Chen, Nickel substrate covered with a Sn-based protection bi-layer as a photoanode substrate for dye-sensitized solar cells, *Electrochim. Acta*, 2013, **99**, 230–237.
56 I. N. Perera, J. M. Pringle, K. Periyapperuma, A. Somers, A. Siriwardana, G. Pozo and C. Pozo-Gonzalo, Enhanced Electrochemical Properties of Cobalt by Varying the Ethylene Glycol - Choline Chloride Composition in a Deep Eutectic Solvent Mixture, *J. Electrochem. Soc.*, 2023, **170**, 5.
57 M. B. Vukmirovic, R. R. Adzic and R. Akolkar, Copper Electrodeposition from Deep Eutectic Solvents---Voltammetric Studies Providing Insights into the Role of Substrate: Platinum vs Glassy Carbon, *J. Phys. Chem. B*, 2020, **124**(26), 5465–5475.
58 S. B. Sadale and P. S. Patil, Nucleation and growth of bismuth thin films onto fluorine-doped tin oxide-coated conducting glass substrates from nitrate solutions, *Solid State Ionics*, 2004, **167**(3), 273–283.
59 V. T. Krasteva and S. P. Papazov, Estimation of current density distribution under electrodes for external defibrillation, *Biomed. Eng. Online*, 2002, **1**(1), 7.
60 D. Bell and A. Garratt-Reed, *Energy Dispersive X-ray Analysis in the Electron Microscope*, Taylor & Francis, 2003.
61 P. Kumar, F. Dinsmore and W. Miao, Hydrogen Bubble-Assisted One-Step Electrodeposition of Cu, Ni, and P toward Electrocatalytic Water Oxidation, *ACS Appl. Energy Mater.*, 2022, **5**(10), 12602–12613.
62 B. H. R. Suryanto, X. Lu, H. M. Chan and C. Zhao, Controlled electrodeposition of cobalt oxides from protic ionic liquids for electrocatalytic water oxidation, *RSC Adv.*, 2013, **3**(43), 20936–20942.